Effects of Ionizing Radiation in Ethylene-Vinyl Alcohol Copolymers and in Composites Containing Microfibrillated Cellulose

Avelina Fernández,[1] M. Dolores Sánchez,[1] Mikael Ankerfors,[2] Jose M. Lagaron[1]

[1]*Institute of Agrochemistry and Food Technology (IATA), CSIC, 46100 Burjassot, Valencia, Spain*
[2]*STFI-Packforsk AB, Box 5604, SE-114 86 Stockholm, Sweden*

Received 24 August 2007; accepted 30 October 2007
DOI 10.1002/app.27709
Published online 20 March 2008 in Wiley InterScience (www.interscience.wiley.com).

ABSTRACT: This study reports on the effect of gamma radiation on morphological, thermal, and water barrier properties of pure ethylene vinyl alcohol copolymers (EVOH29 and EVOH44) and its biocomposites with the nanofiller microfibrillated cellulose (2 wt %). Added microfibrillated cellulose (MFC) preserved the transparency of EVOH films but led to a decrease in water barrier properties. Gamma irradiation at low (30 kGy) and high doses (60 kGy) caused some irreversible changes in the phase morphology of EVOH29 and EVOH44 copolymers that could be associated to crosslinking and other chemical alterations. Additionally, the EVOH copolymers and the EVOH composites reduced the number of hygroscopic hydroxyl functionalities during the irradiation processing and novel carbonyl based chemistry was, in turn, detected. As a result of the above alterations, the water barrier properties of both neat materials and composites irradiated at low doses were notably enhanced, counteracting the detrimental effect on water barrier of adding MFC to the EVOH matrix. © 2008 Wiley Periodicals, Inc. J Appl Polym Sci 109: 126–134, 2008

Key words: EVOH; EVOH composites; irradiation; water barrier; microfibrillated cellulose

INTRODUCTION

Ethylene vinyl alcohol copolymers (EVOH) are random semicrystalline materials with excellent barrier properties to gases and food aroma compounds. They are produced via saponification of ethylene-*co*-vinyl acetate copolymers where the acetoxy group is converted into a secondary alcohol. These materials are increasingly used in the food packaging industry, especially in multilayer packaging. However, barrier and mechanical properties of EVOH suffer from water contact due to water uptake and the associated swelling ratio.[1] EVOH crystallinity and performances have been conveniently enhanced by adding, for example, low amounts of organoclays.[2,3] Microfibrillated cellulose (MFC) from wood pulp is a reinforcing filler with excellent potential to be used in polymer composites. The MFC material consists of long nanoscale bundles of microfibrills, which form entangled networks. MFC is normally prepared by the delamination of delignified wood fibers in high-pressure homogenizers; the diameter of the MFC from Scandinavian softwood pulp is $\sim$ 17–30 nm.[4] This filler is being currently studied to increase the amount of sustainable components in the formulation of plastics, and to provide additional benefits related to the mechanical and barrier properties of the films. Thus, MFC has been reported to have an acceptably high aspect ratio and, in general, the composites with cellulose derived materials have been observed to improve the mechanical properties of polymer films.[4–7] However, its hydrophilic nature may diminish the composites performances in contact with moisture, and therefore have to be carefully investigated.

Gamma irradiation is not only used for material sterilization but also to improve the properties of polymers and in aseptic packaging technologies.[8] Typical effects of irradiation in polymers are chain scission associated to the formation of free radicals and low molecular weight radiolysis compounds, and finally crosslinking[9]. Changes in permeation and mechanical properties due to crosslinking might improve the performances of plastics for instance storage of packaged food at low doses,[10,11] and usually mechanical properties are only affected by high radiation doses.[11] The formation of free radicals and low-molecular-weight compounds might generate undesirable off-flavors or discolorations in the plastics, which could impair the use of this treatment during processing of packaged foods.

Correspondence to: J. M. Lagaron (lagaron@iata.csic.es).
Contract grant sponsor: CYCIT project; contract grant number: MAT2003-08,480-C3.
Contract grant sponsor: EU integrated project SUSTAINPACK.
Contract grant sponsor: MEC; contract grant number: MAT2006-10261-C03.

Irradiated EVOH copolymers have been investigated as candidates for food contact, and good perspectives were reported, since EVOH has not generated detectable radiolytic nonvolatile compounds in food simulants.[12] Furthermore, in food contact materials, permeation properties are probably the most relevant characteristics to be ascertained and controlled. Thus, a previous work in our lab reported[13] that oxygen scavenging properties can be triggered by irradiation of an EVOH copolymer containing 29 mol % of vinyl alcohol. Additionally, a decrease in oxygen permeability depending on the irradiation dose of some EVOH based materials was reported.[14] The mechanical rigidity was not strongly affected by irradiation up to 30 kGy, or was even slightly improved due to crosslinking.[13,14] Both works revealed the presence of low amounts of volatiles, mainly aldehydes and ketones, after irradiation of EVOH based materials at radiation doses up to 30 or 90 kGy.

This work reports on the impact of EVOH nanocomposite materials containing a renewable cellulose based nanofiller, through the characterization of morphological, thermal, and water permeation properties, and explores the possibility of improving composite water barrier performances using an ionizing radiation source.

MATERIALS AND METHODS

Materials

Commercial grades (Soarnol® standard grades: EVOH2903 and EVOH4403) of ethylene-vinyl alcohol copolymers containing a 29 or a 44 mol percentage of ethylene in the composition, respectively, were supplied by Nippon Synthetic Chemical Industry (Nippon Goshei, Osaka, Japan). MFC was kindly provided by STFI Packforsk AB (Stockholm, Sweden) in a gel-like form (2 wt %). MFC microfibrills were characterized by STFI to be 10–30 nm width, and 0.7–1 μm length. Further details of material preparation and characterization can be found elsewhere.[4]

Since the MFC is a gel-like system, dissolution and solvent-evaporation route (so-called casting) was followed. Thus, solvent cast film samples of the EVOH2903 (EVOH29) and of the EVOH4403 (EVOH44) materials with 2 wt % fiber contents were prepared using isopropanol : water (70 : 30) as a solvent. The polymer-fiber solutions were stirred in a reflux at 100°C for 90 min and subsequently cast onto Petri dishes to generate films after solvent evaporation at 80°C of around 100 μm thickness.

Ionization treatments

Ionization was carried out in a Rhodotron (IBA, Belgium) circular electron accelerator (Ionmed, Tarancón, Spain) in the presence of air at room temperature. Treatment lots were deposited in a transporting trade leading to the electron beam. Radiochromic dosimeters (1 cm × 1 cm) FTW-60.0 (Far West Technology, CA) were employed, and the absorbed dose was measured at 600 nm in a spectrophotometer Genesys-5 (Espectronic, NY) with an uncertainty of 0.006 for a confidence level of 95%. Minimum doses applied were 32.1 and 63.6 kGy. Thereafter samples were labeled as 30 and 60 kGy. Nonionized samples were separated as controls. Further information of the set-up can be found at http://www.ionmed.es.

Optical light polarized microscopy

Polarized light microscopy (PLM) examinations were made on the samples using an ECLIPSE E800-Nikon (Kanagawa, Japan) with a capture camera DXM1200F-Nikon.

Scanning electron microscopy

Scanning electron microscopy (SEM) was performed after samples were cryofractured in liquid nitrogen, mounted on bevel sample holders and sputtered with Au/Pd in a vacuum. The SEM pictures were obtained using a Hitachi S4100 (Hitachi High Technologies, Wokingham, UK) and were taken with an accelerating voltage of 10 keV on the sample thickness.

Atomic force microscopy

Atomic force microscopy (AFM) measurements were performed using a NanoScope IIIa (Digital Instruments, Tucson, AZ) to investigate the morphology of the fiber surfaces in the films of the biocomposites. The images were scanned in tapping mode in air using commercial Si cantilevers (Digital Instruments) with a resonance frequency of 320 kHz. Images of at least four different areas were scanned for each sample. AFM data in this article show typical morphologies observed.

Differential scanning calorimetry

The thermal properties of EVOH29 and EVOH44 and their composites with MFC were analyzed using a Perkin–Elmer DSC 7 thermal analysis system (Waltham, MA). The materials were scanned at a speed of 10°C/min from room temperature up to 10°C over the melting point. The samples for DSC analysis were ~ 5 mg. Previous to evaluation, the thermal runs were subtracted analogous runs of an empty pan. The DSC equipment was calibrated using indium as a standard. DSC analysis was performed in duplicate.

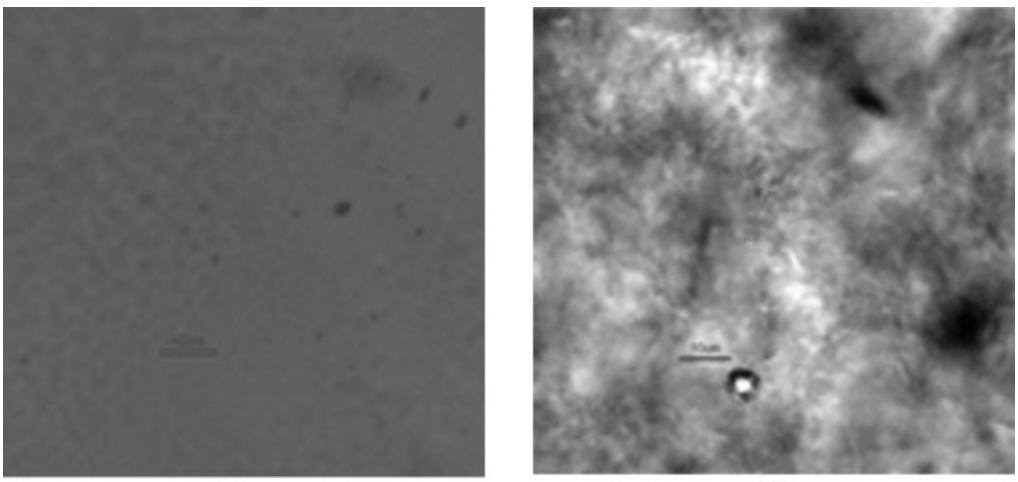

Figure 1 Polarized light images of EVOH44 (a) and of EVOH44 containing 2 wt % of MFC (b). Scale bars are 10 μm in the Figures.

Raman spectroscopy

Raman spectra were taken with a Jasco NRS-3100 Confocal Micro-Raman spectrophotometer (Jasco, Easton, MD), which provides high laser spot lateral and depth sample resolutions, i.e., measured samples areas are smaller than 2 μm when the optimum confocal instrumental setup is selected and using a 100× short working distance microscope objective. The laser source used was a red light tuned at 632.8 nm and powered at 12.4 mW.

Fourier transform infrared spectroscopy

Transmission and attenuated total reflection (ATR) Fourier transform infrared spectra were recorded with a Bruker Tensor 37 equipment (Bruker GmbH, Ettlingen, Germany) with 4 cm^{-1} resolution and 4 s as typical acquisition time. Previous FTIR recordings, the samples were dried at 80°C for 48 h. Results were recorded in duplicate.

Water desorption

Samples were dried in an oven at 80°C for 24 h. They were then allowed to saturate in water inside a desiccator at 100% RH and were later placed in a desiccator at 0% RH and monitored during desorption until constant weight (indicating equilibrium desorption).

The diffusion coefficient of water was estimated from the desorption curves by means of weight loss experiments using an analytical balance Voyager® V11140. The detailed procedure was carried out as follows: At water sorption saturation conditions—defined as the point where consecutive weighing experiments yielded equal values—of the specimens dipped in the compound, the samples were carefully blotted with a tissue to remove the excess of water vapor condensed over the film surface (this step is considered as time zero) and were periodically weighted until they yielded constant weight. D values were estimated by fitting the experimental data versus time during desorption experiments to the first six sum terms of the corresponding solution of Fick's second law [eq. (1)]. Experiments were done in triplicate.

$$\frac{M_t}{M_e} = \frac{8}{\pi^2}\sum_{n=0}^{\infty}\frac{1}{(2n+1)^2}\exp\left\{\frac{-D(2n+1)^2\pi^2 t}{l^2}\right\} \quad (1)$$

Solubility (S), required to estimate the permeability, was estimated from the water uptake at equilibrium, the density of the materials and the water vapor partial pressure at 24°C. The validity of the step-wise method was assessed by *in situ* continuous desorption experiments followed by ATR-FTIR spectroscopy (results not shown).

Statistical analysis

One-way analysis of variance (ANOVA) was performed with XLSTAT-Pro (Win) 7.5.3 (Addinsoft, NY). Statistical analysis was run with a confidence level of 95%. Comparisons between treatments were evaluated with the Tukey test.

RESULTS AND DISCUSSION

Composites morphology

Visual observations of EVOH29 and EVOH44 composite films indicated that the samples were transparent, suggesting that a satisfactory dispersion of the filler was achieved in the films. This observation was also confirmed by polarized light optical microscopy as reported in Figure 1. The MFC microfibrils

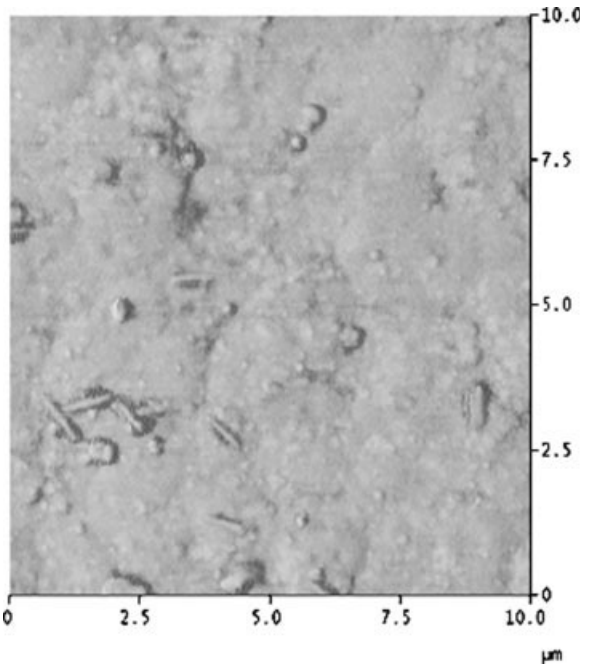

Figure 2 Atomic force microscope image of EVOH29 containing 2 wt % of MFC.

were seen to be well dispersed across the sample thickness, albeit some MFC agglomeration may also take place in certain sample areas. Further examination of the film surface by AFM (Fig. 2) typically revealed the presence of some MFC fibers that remained at the nanolevel after casting, and showed typical fiber diameters of 30–70 nm, in concordance with the reported morphology data for the MFC. Fiber length was confirmed to be around 1 μm, also typical for MFC fibers, and the filler tended to have a regular shape at the film surface.

Furthermore, at least five SEM images of cryofractured MFC microfibrills were analyzed for each film source. Figure 3 again suggests that a reasonably good dispersion and an excellent interfacial adhesion of cellulose MFC microfibrills in the EVOH matrix must have been achieved, since typically MFC microfibrills could not be discerned from the matrix in the SEM observations. Observations in the irradiated samples by the same techniques did not reveal detectable morphological changes as a result of the irradiation process. A previous work using highly purified α-cellulose microfibers in biopolyesters reported that at low fiber concentrations, the cast films retained the optical properties, had good fiber dispersion, and even induced improvements in barrier properties to gases and vapors.[6] A similar work used MFC to reinforce the properties of the polar matrix amylopeptine.[4] The latter system studied is perhaps closer to the one described here because amylopeptine is a highly hygroscopic biopolymer that exhibit similar properties as EVOH. This study showed that the MFC dispersed rather well in the polar biopolymer and led without the need for plasticizers to improvements in stiffness without inducing material brittleness.

Thermal analysis

Melting temperature (T_m) and heat of fusion (ΔH_m) for EVOH and EVOH composites with MFC were determined from the DSC first and second heating runs. Plain results were normalized by the amount of EVOH in the composites. Two replicates were analyzed, differences between the recorded values were always below 2%.

Results for cast films irradiated and nonirradiated are summarized in Table I and some representative thermograms are shown in Figure 4 for comparison purposes. The addition of 2% of MFC did not greatly alter the melting points of EVOH29 or EVOH44 in cast films during the first and second heating runs. However, the melting point was generally lower in irradiated samples, with or without added MFC microfibrills, showing a small but constant trend in the effects of irradiation on the EVOH thermal properties, probably due to molecular alterations caused by chemical and physical changes. The melting point drop is usually interpreted as a result of the creation of a more defective and/or smaller in size EVOH crystalline morphology after irradiation[13] and the effects of crosslinking in EVOH29 irradiated up to 30 kGy have already been described.[14] The latter process was reported to generate a lower free volume amorphous phase and the authors also claimed that smaller crystallites were formed. Nevertheless, the presence of a different chemistry and/or or bulkier groups unable to crystallize or cocrystallize does also alter or impair the proper development of crystallinity after melting and recrystallization as observed (see below).

Melting enthalpy in the first heating run was constantly lower in samples of EVOH29 and EVOH44 containing MFC, compared to the nonirradiated controls. High MFC dispersion and possibly interfacial adhesion by hydrogen bonding could hinder to some extent the lateral rearrangements in polymer chains, and hence crystallization in the materials. Surprisingly, irradiation appeared to revert the effects seen in the melting enthalpy and samples containing MFC showed a heat of fusion in the first heating run closer to the untreated control with no MFC. This is possibly the result of an irradiation-induced local temperature rise resulting in annealing for the crystalline morphology. Thus, an annealing effect over the crystalline morphology,[9] similar to those previously reported by thermal treatments below the melting point of EVOH materials[1] cannot be discarded.

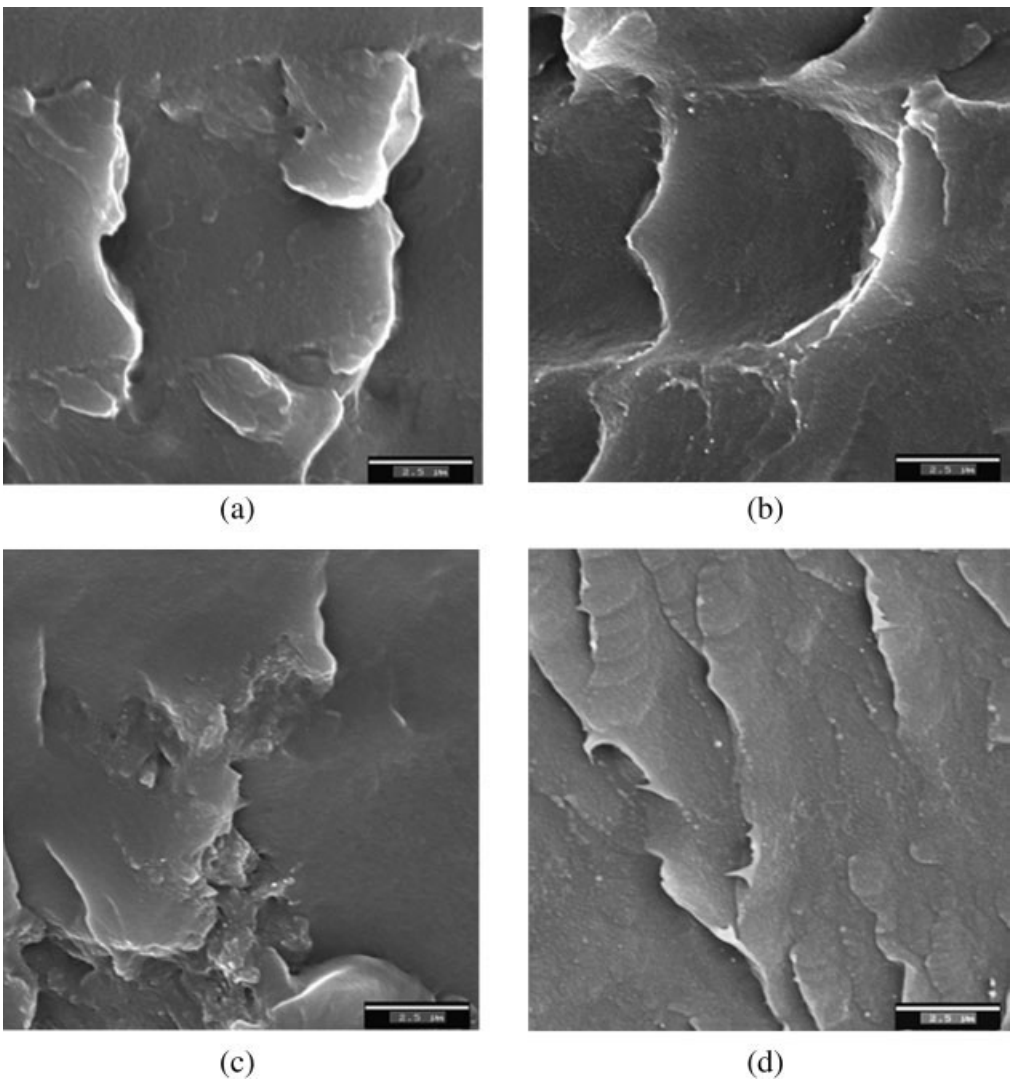

Figure 3 Micrographs of EVOH and EVOH composites containing 2 wt % of MFC obtained with a scanning electronic microscope. (a) EVOH29; (b) EVOH44; (c) EVOH29 with 2 wt % of MFC; (d) EVOH44 with 2 wt % of MFC. Scale bars are 2.5 μm.

The maximum of the crystallization peak after the first melting run was very similar for all the mixtures and, therefore, irradiation appeared not to have a detectable trend over the degree of undercooling needed for the crystallization of EVOH, or over the crystallization kinetics of the material. Nevertheless, the crystallization enthalpy of both neat copolymers was recorded to be lower after irradiation, hence suggesting alterations in the EVOH crystallization process due to the chemical changes occurring in the polymer, as reported below. Those effects, added to the fact that MFC probably interfered with the crystallization process, caused some decrease in the crystallization enthalpy of the composites compared to the neat materials.

The second heating run also revealed small differences in the melting temperature and in the melting enthalpy, with a tendency similar to the one observed for the first heating run: lower T_m and ΔH_m in irradiated samples. This points out that irradiation might eventually lead to some permanent structural effects in the crystalline morphology for EVOH neat and composite materials that must be associated to chemical changes and crosslinking in the lateral order, as already suggested to happen for EVOH29[4] copolymers and for other polymers.[12]

Raman spectroscopy

Typical vibrational bands previously described for EVOH materials[15] were identified in all irradiated and nonirradiated samples. The bands at 2900 cm^{-1} and the shoulder at 2840 cm^{-1} were previously associated to the skeletal CH and CH_2 vibrations.[14] The ratio C—H to O—H bonds increased with increasing the ethylene content and bands associated to CH_2 group vibrations were therefore enhanced in EVOH44 compared to EVOH29 copolymers. The rel-

TABLE I
Thermal Analysis of EVOH and EVOH Composites as a Function of Irradiation Absorbed Doses (30 or 60 kGy)

			Pure	30 kGy	60 kGy	2%f	2% 30 kGy	2% 60 kGy
EVOH29	1st Heating run	T_m	188.4	187.2	186.9	188.5	188.5	186.9
		ΔH_m	68.6	65.6	68.9	66.6	70.2	68.6
		Width	16.5	17.3	18.1	16.5	13.6	12.2
	1st Cooling run	T_c	163.1	162.4	162.2	161.9	161.7	161.4
		ΔH_c	−75.1	−63.5	−65.2	−50.1	−57.3	−53.9
		Width	6.1	6.7	7.0	9.1	9.4	4.8
	2nd Heating run	T_m	189.3	188.5	188.0	189.4	188.6	187.6
		ΔH_m	59.8	53.6	54.9	58.5	54.7	52.9
		Width	8.5	10.1	10.6	9.2	10.1	9.3
EVOH44	1st Heating run	T_m	162.5	162.3	161.1	162.5	161.9	161.8
		ΔH_m	61.0	59.6	58.2	53.2	60.6	60.0
		Width	15.3	15.2	17.9	16.6	15.8	16.4
	1st Cooling run	T_c	139.5	139.4	139.4	139.1	140.1	138.9
		ΔH_c	−55.2	−54.9	−52.9	−54.4	−53.1	−51.7
		Width	7.9	8.2	8.0	10.0	8.0	9.1
	2nd Heating run	T_m	164.5	163.5	162.6	164.3	163.0	162.4
		ΔH_m	49.1	47.2	44.2	48.5	45.2	43.3
		Width	8.0	9.2	9.5	8.3	8.8	9.9

Melting and crystallization temperatures (T_m and T_c, respectively) were expressed in °C; melting and crystallization enthalpy (H_m and H_c, respectively) were expressed in J g^{-1}. The results are the mean of two replicates.

ative intensity with regard to the band at 2900 cm^{-1} remained fairly constant for all the samples, indicating that structural alterations due to irradiation have not affected to a remarkable extent the skeletal Raman spectrum of the materials.

Most differences were accounted at lower energy levels, in the range between 1500 and 700 cm^{-1}, where band assignments are typically more difficult to assign. Thus, the already described bending vibrations of CH and OH around 1293 cm^{-1}, the bending of C=O and OH groups at around 1134 cm^{-1}, the C=O stretching band at around 1065 cm^{-1}, and the skeletal vibrations between 800 and 1000 cm^{-1} remained fairly constant in the composites and in the irradiated samples. Significant differences were found between both neat polymers in this spectral range since the shoulder between the 1134 and the 1065 cm^{-1} bands was more clearly defined in the EVOH44 copolymers and composites than for EVOH29 (Fig. 5), reflecting structural differences that likely arise from the difference in the fraction of vinyl alcohol in the copolymer. Small frequency shifts of Raman lines to lower wavenumbers could be observed suggesting rearrangements in the EVOH skeleton as a result of the chemical and physical alterations undergone upon irradiation.

Two characteristic bands were detected at ~ 1332 and 1225 cm^{-1} in the nonirradiated composites (Fig. 5). The band at ~ 1332 cm^{-1} probably arises from the EVOH structure, since it is slightly displaced in position in EVOH29 compared to EVOH44 (results not shown) and can be clearly observed in neat EVOH44 (Fig. 5). This band seems to be more pronounced in the composites possibly due to the interaction

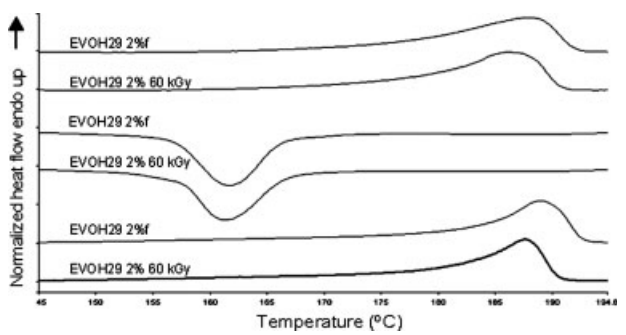

Figure 4 DSC thermograms of, from top to bottom, first heating scan, crystallization scan, and reheating scan of EVOH29 composites containing 2 wt % of MFC untreated (upper curves) and irradiated at 60 kGy (lower curves).

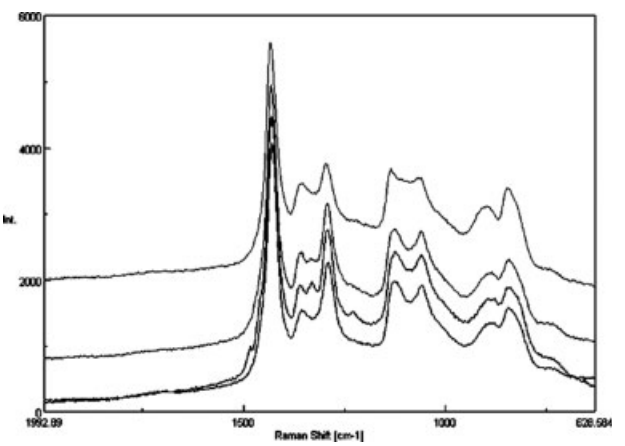

Figure 5 Raman spectra of, from top to bottom, EVOH29, EVOH44, EVOH44 with 2 wt % of MFC, EVOH44 treated at 60 kGy and EVOH44 with 2 wt % of MFC treated at 60 kGy.

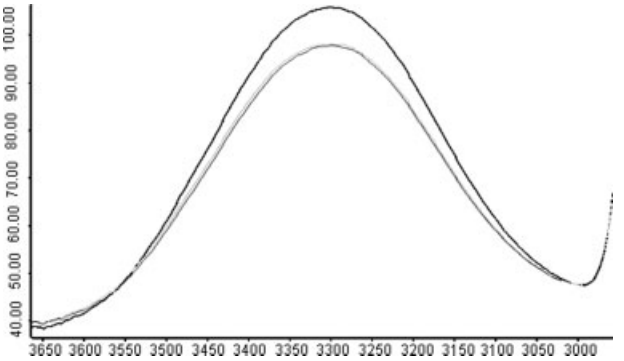

Figure 6 Normalized (to the intensity of the CH_2 symmetric stretching band at 2855 cm^{-1}) intensity in the OH stretching band at 3300 cm^{-1} of EVOH29 for untreated (higher intensity peak) and irradiated to 30 and 60 KGy (lower intensity peaks) samples.

between the EVOH C—O groups and the MFC polar chemistry. In this frequency range, also some stretching and bending modes of cellulose might be expected, generating peaks that overlap with the ones of EVOH materials and perhaps giving rise to the scattering in this spectral range. Nevertheless, the intensity of this band at 1332 cm^{-1} decreases in both EVOH29 and EVOH44 composites after irradiation, as observed in Figure 5 for EVOH44, indicating that its assignment could be related to C—O bonds as observed in our experiments with FTIR spectroscopy. These findings suggest changes in the chemical environment of this groups that cannot be readily assigned or confirmed due to the limited existing information regarding the Raman spectra of EVOH materials. No other bands attributed by other authors[16] to potential interactions with cellulose could be identified during our research.

Fourier transformed infrared spectroscopy

Fourier transform infrared spectroscopy was used in transmission and in ATR modes to further study the effects of irradiation on the chemical structure of EVOH29 and EVOH44 composites.

In the ATR-FTIR experiments, the spectra of dried samples were normalized to the CH_2 symmetric stretching band at 2855 cm^{-1}. This band is assumed to remain unmodified during the processing of the samples described here and has, therefore, been used as an internal standard for the experiments as reported earlier.[1]

The normalized intensity of the OH stretching band centered at 3300 cm^{-1} and associated, in dried samples, to the presence of OH groups from the vinyl alcohol part of the copolymer structure and to some extend to the MFC, is shown in Figure 6 for the composite of EVOH29 as an example. The effect of irradiation at 30 or 60 kGy results in an apparent decrease in the intensity of the OH band of the polymer. This observation has never been reported, although, it has always been suspected from earlier work.[13] The hydroxyl groups of the composites were similarly affected by effects that could be attributed to the irradiation-induced transformation of a certain amount of hydroxyl groups into, among other chemistry, carbonyl based chemistry. This fact could be further confirmed by transmission FTIR spectroscopy, as reported below.

The changes previously associated[13] to the C=O stretching mode of aldehydes and ketones between 1680 and 1750 cm^{-1} can only be weakly discerned in the ATR mode of irradiated neat materials and composites and were, therefore, studied further in the transmission mode. The transmission mode allows a better observation in relatively thick samples of small absorbance bands. Thus, while, due to excessive thickness of the specimens, most bands give superabsorbance, three weak bands with maxima at 1760, 1736, and 1711 cm^{-1} can be clearly observed which are thought to arise from C=O groups primary coming from uncomplete saponification during the synthesis of EVOH (see Figs. 7 and 8). After irradiation, the intensity of the three bands was seen higher [see Fig. 7(a,b)] than in untreated controls, reflecting the upcoming in carbonyl groups due to irradiation in both polymers, EVOH29 and EVOH44. Formation of carbonyl groups partially coming from hydroxyl transformation, as detected by ATR in the 3300 cm^{-1} intensity band and/or by radical chemistry within the polymers, seemed to be more relevant

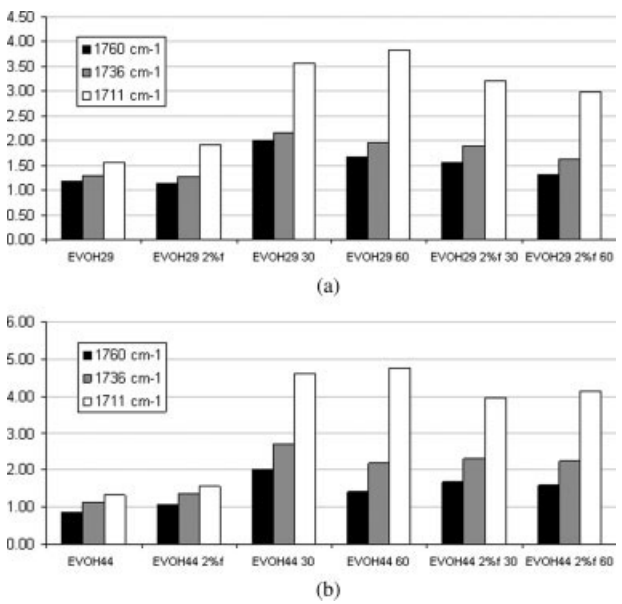

Figure 7 Relative intensities normalized by sample thickness in mm, of the absorbance of the three C=O stretching bands for EVOH29 (a) and EVOH44 (b) and their composites containing 2 wt % of MFC.

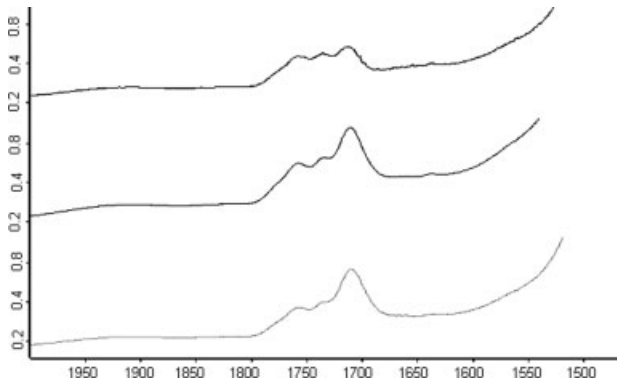

Figure 8 FTIR spectra in the 2000–1550 cm^{-1} range of, from top to bottom, EVOH29, EVOH29 irradiated at 30 kGy, and EVOH29 irradiated at 60 kGy.

both in EVOH44 and EVOH44 composites, comparing the intensity of the bands in Figure 7(a,b). Other authors reported already similar results for irradiated EVOH; for example, after irradiation of multilayer films containing PET/PE/EVOH/PE several newly formed unsaturated hydrocarbons, alcohols, aldehydes, and ketones were detected,[17] in a similar way as reported in other works,[13,14] pointing to oxidation or free radical formation, as well as leading to the formation of certain volatiles.

Water barrier properties

The water transport properties of EVOH films and EVOH composites were followed during water sorption and subsequent desorption to relate the observed morphological and chemical changes to the barrier behavior.

The gravimetric water uptake accounted for ~ 12–13 wt % in EVOH29 and ~ 6–7 wt % in EVOH44 samples. Irradiated samples tended to show slightly lower uptake values but all changes were within 1 wt % for both samples and within the measurement error indicating that changes in water solubility are smaller in the samples. After reaching equilibrium the samples were allowed to desorb under dry conditions in a desiccator (at 0% RH). The corresponding estimated diffusion (D) and indirect permeability (P) coefficients are reported in Table II.

From Table II the untreated composites showed higher diffusion rates than the unfilled materials. This also led to a higher permeability for the composites. The reason for the increase in diffusion and permeability in the composites could be ascribed to the hydrophilic character of the MFC but, since the solubility was not clearly enhanced, it is most likely ascribed to morphological changes reported along this work. Those were mainly changes in crystallinity and in the phase morphology promoted by the MFC filler.

Table II also shows that the irradiated samples exhibit a significant reduction in the water diffusion coefficient, and additionally, in permeability values. Consequently, a more compact crystalline structure due to crosslinking, and the decrease in the number of the strongly hydrophilic OH groups, as observed by ATR, are thought to be responsible for this behavior in the irradiated EVOH and EVOH composites. For example, a reduction in the water diffusion coefficient of ~ 54% was observed in the EVOH29 at 60 kGy and of ~ 44% in the EVOH44 at 30 kGy, compared with their nonirradiated counterparts. Moreover, permeability values for the irradiated neat EVOH29 (5.72 or 2.57 $\times$ 10^{-15} kg m s^{-1} m^{-2} Pa^{-1} at 30/60 kGy respectively) and EVOH44 (0.61 or 0.86 $\times$ 10^{-15} kg m s^{-1} m^{-2} Pa^{-1} at 30/60 kGy, respectively) films were considerably lower than the calculated permeability for the nontreated counterparts, confirming the remarkable effect of irradiation in reducing water transport in the materials.

Additionally, in most cases, the gamma irradiation of composites with cellulose at 30 kGy reverted the negative barrier effect generated by blending with the MFC filler, as the composites showed for EVOH29 and EVOH44 lower water diffusion coefficient (~ 32 and 7%, respectively) than the unfilled materials. Permeability values were also remarkably improved for irradiated EVOH29 composites (3.52 $\times$ 10^{-15} kg m s^{-1} m^{-2} Pa^{-1}), confirming enhanced barrier properties in irradiated EVOH29 composites compared to the neat nonirradiated EVOH29 films. The permeability of EVOH44 composites (1.12 $\times$ 10^{-15} kg m s^{-1} m^{-2} Pa^{-1}) also showed slightly better barrier values than the nonirradiated EVOH44 composites, but the improvement was in this case not sufficient to completely counteract the effect of adding MFC. The authors are currently measuring

TABLE II
Diffusion (D, m^2 s^{-1}) and Permeability (P, kg m s^{-1} m^{-2} Pa^{-1}) Coefficients of Water in EVOH and EVOH Composites Untreated and Irradiated with 30 and 60 kGy

	D Mean ($\times 10^{-13}$)	P Mean ($\times 10^{-15}$)
EVOH29	1.16^{ab}	6.37
EVOH29 2%f	1.73^{a}	8.88
EVOH29 30	1.09^{ab}	5.72
EVOH29 60	0.53^{b}	2.57
EVOH29 2%f 30	0.79^{ab}	3.52
EVOH29 2%f 60	1.59^{a}	7.83
EVOH44	0.46^{cd}	1.14
EVOH44 2%f	0.50^{cd}	1.39
EVOH44 30	0.26^{d}	0.61
EVOH44 60	0.33^{d}	0.86
EVOH44 2%f 30	0.43^{cd}	1.12
EVOH44 2%f 60	0.81^{c}	1.95

The results are the mean of three replicates. Within the D column, means with different superscripts are significantly different ($P < 0.05$).

mechanical and other properties such as chemicals release from the irradiated materials but only small changes in mechanical and physicochemical properties of multilayer commercial plastics containing EVOH treated at 30 kGy have been previously reported.[18]

The gamma irradiation of composites with MFC at 60 kGy usually led to films with barrier performances that were either not too different or even worse than those of the untreated composites. Thus, the water diffusion coefficient and permeability values of EVOH44 composites at 60 kGy were remarkably higher ($D \sim 150\%$ over the values of the neat materials) than the barrier properties measured for its nonirradiated counterpart, confirming that 60 kGy is a deleterious dose in terms of improving barrier properties. Stark negative effects of high radiation doses up to 100 kGy have been reported for other materials.[11]

Previous works have pointed out that irradiated materials undergo crosslinking processes at low radiation doses and that this phenomenon could be linked to slight reductions in gas and water vapor transmission rates possibly due to reductions in free volume.[19,14] Moreover, another work showed that a certain local increase in the sample temperature can take place as a result of this treatment.[9] This process could be responsible for a certain annealing effect in the neat and the more distorted composite samples, promoting the formation of more robust crystalline structures leading to a certain improvement in barrier properties. Finally, a decrease in polar groups due to irradiation was also found in this study, which would in principle lead to a decrease in the hydrophilic nature of the polymer.

Only doses lower than 30 kGy are typically recommended or authorized for in-package pasteurization of goods. In this context, the results reported here indicate that 30 kGy can be of sufficient interest to at least enhance the water barrier properties of the highly hydrophilic EVOH copolymers and biobased composites.

CONCLUDING REMARKS

Gamma irradiation caused diverse chemical modifications in EVOH29 and EVOH44 copolymers, and in their composites with cellulose; those changes led to morphological modifications. The generated structures differed slightly in the amount and size of crystals and lost OH groups, while a raise in carbonyl groups could be recognized. A positive annealing effect of irradiation could be inferred, and the water barrier properties of the irradiated materials were notably enhanced if the radiation did not exceed a deleterious doses. The composites of EVOH and MFC did not show better water barrier properties than the pure material probably due to defects in crystallinity induced by the cellulose bulk, but composite properties were positively improved if low radiation doses were applied. MFC from renewable sources is a good candidate to become a filler for EVOH materials, and to obtain similar or better performances, additional treatments, as irradiation, might have to be applied.

References

1. Lopez-Rubio, A.; Lagaron, J. M.; Gimenez, E.; Cava, D.; Hernandez-Munoz, P.; Yamamoto, T.; Gavara, R. Macromolecules 2003, 36, 9467.
2. Jeong, H. M.; Kim, B. C.; Kim, E. H. J Mater Sci 2005, 40, 3783.
3. Cabedo, L.; Gimenez, E.; Lagaron, J. M.; Gavara, R.; Saura, J. J. Polymer 2004, 45, 5233.
4. López-Rubio, A.; Lagaron, J. M.; Ankerfors, M.; Lindström, T.; Nordqvist, D.; Mattozzi, A.; Hedenqvist, M. S. Carbohydr Polym 2007, 68, 718.
5. Nakagaito, A. N.; Yano, H. Appl Phys A 2005, 80, 155.
6. Sánchez-García, M. D.; Giménez, E.; Lagarón, J. M. Carbohydr Polym 2007, 71, 235.
7. Fendler, A.; Villanueva, M. P.; Gimenez, E.; Lagaron, J. M. Cellulose 2007, 14, 427.
8. Diehl, J. F. Radiat Phys Chem 2002, 63, 211.
9. Rouif, S. Meth Phys Res B 2005, 236, 68.
10. Klemchuk, P. P. Radiat Phys Chem 1993, 41, 165.
11. Zenkiewicz, M. Radiat Phys Chem 2004, 69, 373.
12. Kothapalli, A.; Sadler, G. Nucl Instrum Methods Phys Res Sect B 2003, 208, 340.
13. Lopez-Rubio, A.; Lagaron, J. M.; Yamamoto, T.; Gavara, R. J Appl Polym Sci 2007, 105, 2676.
14. Byun, Y. J.; Hong, S. I.; Kim, K. B.; Jeon, D. M.; Kim, J. M.; Whiteside, W. S.; Park, H. J. Radiat Phys Chem 2007, 76, 974.
15. Cooney, T. F.; Wang, L.; Sharma, S. K.; Gauldie, R. W.; Montana, A. J Polym Sci Part B: Polym Phys 1994, 32, 1163.
16. Schenzel, K.; Fischer, S.; Brendler, E. Cellulose 2005, 12, 223.
17. Riganakos, K. A.; Koller, W. D.; Ehlermann, D. A. E.; Kontominas, M. G. Radiat Phys Chem 1999, 54, 527.
18. Goulas, A. E.; Riganakos, K. A.; Kontominas, M. G. Radiat Phys Chem 2003, 68, 865.
19. Robertson, G. L. Permeability of Thermoplastic Polymers. Food Packaging: Principles and Practice; Marcel Dekker: New York, 1993; p 73.